

where $\text{int}(x)$ denotes the integer part of the number x . The presence of this function represents an idealization due to the assumption that the assumed source has an abrupt edge and turns on instantaneously. At early times the argument of the integer function is less than and the distribution is similar to that for the impulsive model (Figure 3). The left-hand edge of the distribution looks like the line described by equation (16), but to the right (larger v_{\parallel}) the distribution is filled in according to the initial distribution f_0 . At later times the dominant features of the distribution are the downgoing (due to the presence of the atmosphere in the opposite leg) and upgoing loss cones (Figure 4). As we show in the next section the loss cones allow maser action to occur.

4. Electron Cyclotron Masers

The theory of electron cyclotron masers has recently been reevaluated and shown to imply higher growth rates under milder conditions than previously thought (Wu and Lee 1979; Hewitt *et al* 1982). Rather than discuss the theory in detail, we mention here only the features needed to investigate the distributions of the preceding section. A single electron is in cyclotron resonance with a wave of frequency ω and wavevector \mathbf{k} at the p -th harmonic if it satisfies the condition

$$\omega - k_{\parallel} v_{\parallel} - p\Omega/\gamma = 0, \quad (21)$$

where k_{\parallel} is the component of the wavevector parallel to the magnetic field, Ω is the local gyrofrequency and $\gamma = (1 - v^2/c^2)^{-1/2}$. The growth rate for a given distribution involves an integral over the contributions of all resonant particles. On the $v_{\perp} - v_{\parallel}$ diagram these particles lie on a half-ellipse given by the solution of (21). Under semirelativistic conditions ($k_{\parallel}c/p\omega \ll 1$) the ellipse becomes a semicircle

$$(v_{\parallel} - v_0)^2 + v_{\perp}^2 = V^2 \quad (22)$$

where v_0 and V are functions of the wave parameters ω and k_{\parallel} (Hewitt *et al* 1982). Thus different circles correspond to different waves. In this limit, the growth rate for a particular wave is just an integral around the appropriate half-circle,

$$\Gamma(p, \omega, \mathbf{k}) = A(p, \omega, \mathbf{k}) \int_0^{\pi} d\phi v_{\perp}^{2p} \frac{\partial f}{\partial v_{\perp}} \quad (23)$$

where A is a function of the wave parameters, $v_{\parallel} = v_0 - V \cos \phi$ and $v_{\perp} = V \sin \phi$. According to (23), growth occurs for any wave whose semicircle lies mostly in regions where $\partial f/\partial v_{\perp} > 0$. If such a circle can be drawn then maser action should take place.

On each of the four figures we have drawn circles whose intersections with the distributions occur in regions in which $\partial f/\partial v_{\perp} > 0$. Thus waves corresponding to these circles should grow. It should be apparent from the general properties of the solutions (in particular, from the shape of (16)) that it is always possible to find such circles at early times, in both of our models. Thus we expect that electron cyclotron maser action should be a common feature during solar flares.

5. Discussion

We have shown that there are two phases in which maser action is likely to occur following a solar flare. In the later

phase, loss cones in upgoing particles develop and are unstable to wave growth, as has been assumed by Holman *et al* (1980) and Melrose and Dulk (1982a). The resulting maser produces radiation at low harmonics.

It is pointed out for the first time here that maser action is also likely to occur in an earlier phase when the particles are predominantly downgoing (e.g. see Figure 1). The resulting maser emits radiation which should be reflected or reabsorbed at a level where its frequency equals the critical frequency for the appropriate mode. The radiation propagates nearly perpendicular to the field lines so heating over a large area is possible. Growth rates in the earlier phase are expected to be high, but so far no detailed calculations for growth rate have been performed for this case.

Once the maser turns on, the distributions are modified through scattering by the radiation. After a number of growth times radiation should reach a level at which significant pitch angle scattering occurs, reducing the value of $\partial f/\partial v_{\perp}$ and tending to switch the maser off. This self-quenching effect of a cyclotron maser corresponds to saturation in a laboratory maser (Melrose and Dulk 1982a).

In conclusion, this study has shown that it is not sufficient to study only masers due to loss cone anisotropies in upgoing particles when investigating radiofrequency heating in flares. Maser emission seems likely to occur in an earlier downgoing phase. The implications of this result have yet to be adequately understood.

References

- Chen Chuan-Le, and R. E. Loughhead, *Proc. Astron. Soc. Aust.*, **5**, (1983).
 Hewitt, R. G., D. B. Melrose, and K. G. Rönmark, *Aust. J. Phys.*, **35**, 447 (1982).
 Holman, G. D., D. Eichler, and M. R. Kundu, in *IAU Symposium 86, Radio Physics of the Sun*, ed. M. Kundu and T. Gergely (Dordrecht: Reidel), p. 205 (1980).
 Melrose, D. B., and G. A. Dulk, *Astrophys. J.*, **259**, 844 (1982a).
 Melrose, D. B., and G. A. Dulk, *Astrophys. J. Lett.*, **259**, L41 (1982b).
 Northrop, T. G., *The Adiabatic Motion of Charged Particles* (Wiley: New York), p. 9 (1963).
 Slottje, C., *Nature*, **275**, 520 (1978).
 Wu, C. S., and L. C. Lee, *Astrophys. J.*, **230**, 621 (1979).

Drifting Subpulses in Pulsars

Michelle C. Allen and D. B. Melrose, *School of Physics, University of Sydney*

1. Introduction

Individual pulses from a given pulsar can differ greatly in both shape and intensity, and are often made up of narrower 'subpulses', i.e. local emission peaks one tenth the width of the mean pulse. Properties such as shape, polarization and

position of subpulses presumably reflect details of the emission processes and of the regions that produce the radiation. An analysis of subpulse properties can be used to gain insight into the fundamental electrodynamic processes occurring near the neutron stars. In this paper we concentrate on one such property of subpulses, namely their drifting, and interpret it in terms of a model of plasma behaviour near the surface of the rotating neutron star.

In Section 2 we summarize the observational characteristics of drifting subpulses. In Section 3 we discuss the relevant properties of the pulsar model of Ruderman and Sutherland (1975, hereinafter RS) on which our model is based. An important point is that the emission region is populated by electron-positron plasma created as a result of a parallel electric field ($\mathbf{E} \cdot \mathbf{B} \neq 0$) building up and discharging near the surface in a quasi-periodic manner. Following a suggestion by Filippenko and Radhakrishnan (1982) we suppose that each discharge leads to the filling of an isolated flux tube with plasma. When filled this flux tube would corotate, but due to the intervening intervals when the parallel electric field grows, its average motion differs from corotation. This motion, which is the basis of our model of the drifting of subpulses is discussed in Section 4. The results of the model are compared with observations in Section 5.

2. Properties of Drifting Subpulses

The position of a subpulse within the pulse profile changes systematically from pulse to pulse. This phenomenon is illustrated in Figure 1. An extensive observational study of subpulse drift was conducted by Oster *et al.* (I-V, 1977-1978) and further work has been done by Bartel *et al.* (1981), Wolszczan (1978, 1980) and Wolszczan *et al.* (1981). On the basis of their results we conclude that the common features of subpulse drift for which any model should account are: —

- i) The drifting phenomenon is common to all subpulses,
- ii) The drift direction is predominantly from the trailing edge

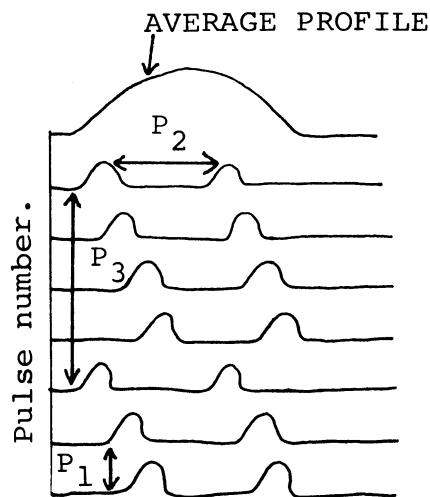


Figure 1. Description of drifting subpulse phenomenon. the pulsar period is P_1 seconds. Subpulses are separated in longitude by P_2 degrees and in time by P_3 seconds.

of the profile to the leading edge and drift is more rapid at the edges of the pulse profile.

- iii) The drift rate is variable and often appears to have two or three preferred values.
- iv) The changes in the drift rate are non-local, i.e. the drift rate of more than one subpulse is altered by whatever causes the change.
- v) There is often strong overlapping of subpulses within a single pulse.
- vi) The period P_3 (cf. Figure 1) is independent of frequency and can vary between $2P_1$ and $15P_1$ where P_1 is the pulse period. The average P_3 value for a pulsar is stable.
- vii) The period P_2 (cf. Figure 1) is independent of P_3 and varies with frequency as does the width of the pulse window. P_2 varies with longitude and is smaller in the leading part of the profile.
- viii) Double profiles (Manchester and Taylor 1977 p. 15) also exhibit the drifting subpulse phenomenon, though serious overlap of subpulses is observed and drift is more marked on the leading edge of the profile.
- ix) Local discontinuities in the subpulse bands are sometimes observed, where the emission is reduced and the drift is slowed down.
- x) The drift rate is slower immediately after a null and increases to its pre-null value over several periods.

3. The Model

It is assumed that pulsars are excellent conductors in both the degenerate interior and the non-degenerate magnetosphere of charged particles. In their conduction regions they possess a corotational electric field satisfying $\mathbf{E}_{cor} + (\boldsymbol{\Omega} \times \mathbf{r}) \times \mathbf{B} = 0$ where $\boldsymbol{\Omega}$ = angular velocity of the star and \mathbf{r} = radius vector from the stellar centre. Thus the space-charge density in the corotating regions $\rho \propto \nabla \cdot \mathbf{E}$ is proportional to $-\boldsymbol{\Omega} \cdot \mathbf{B}$ (Goldreich and Julian, 1969).

An essentially dipolar magnetic field is assumed and as in the RS model an oblique rotator whose magnetic axis is antiparallel (as opposed to parallel) to the rotation axis is considered. The region of 'open' magnetic field lines (RS) is positively charged. Particles streaming along open field lines escape from the magnetosphere and as positive charge cannot be supplied by the surface the magnetosphere lifts off from the surface, forming a growing gap in which $\mathbf{E} \cdot \mathbf{B} \neq 0$. The potential difference between the top of the gap and the star grows as h^2 where h = height of the gap. Eventually the gap is discharged by an avalanche of electron-positron pairs. The $\mathbf{E} \cdot \mathbf{B}$ that has built up falls to zero as the sparking region becomes filled with plasma and this is thought to inhibit the growth of another simultaneous discharge within a distance $\sim h$ on the surface of the star. Thus the polar cap gap is discharged in a number of discrete sparks and the radiation produced above the discrete sparking regions is observed as subpulses.

During the discharge positrons are accelerated outwards and electrons inwards. (It is not clear in the RS model how a charge buildup on the star is avoided).

For a particle on a given field line to corotate with the neutron star, one requires $\mathbf{E} = -(\boldsymbol{\Omega} \times \mathbf{r}) \times \mathbf{B}$ where \mathbf{B} is the magnetic field at the point in question and \mathbf{r} is the radius

vector to the point. This condition holds for regions connected to the neutron star by magnetic field lines all along which $\mathbf{E} \cdot \mathbf{B} = 0$ (RS, Appendix). When a magnetospheric gap is present $\mathbf{E} \cdot \mathbf{B} \neq 0$ for field lines penetrating the gap and so the electric field required for corotation is not established on such field lines at points further from the star. Particles in such regions can drift relative to the star with drift velocity

$$v_{ED} = \frac{\Delta \mathbf{E} \times \mathbf{B}}{|\mathbf{B}|^2} \quad (1)$$

where $\Delta \mathbf{E}$ is the difference between the actual electric field and the co-rotational electric field. This is the cause of subpulse drift. RS did not explain the mechanism by which $\Delta \mathbf{E}$ is generated. We assume that $\Delta \mathbf{E}$ is established by a separation of charges.

RS assumed that the discharge is quasi-steady, the implication being that discharges may never entirely cease and that although gaps may oscillate in size, they may never disappear altogether. This assumption leads to incorrect estimates of the drift rate (Oster *et al.* III, 1976). In our model we assume the discharge occurs in a quasi-periodic manner with a cycle time $\approx 1 \times 10^{-5}$ s (RS) but with the electric contact with the star broken only for a fraction of this time. A gap of height $h \sim 150$ m (RS) grows (at the speed of light) in $\approx 5 \times 10^7$ s and then discharges. Thus only for $\approx 1/20$ of the sparking cycle does corotation break down as $\mathbf{E} \cdot \mathbf{B} \neq 0$.

When the rotation and magnetic axes are aligned, sparking regions drift in circular paths around the magnetic pole. RS assumed that the drift path in the non-aligned case is also around the magnetic pole. It is shown below that a more likely possibility is that the drift path is in the same direction as the corotation path.

4. Flux Tubes and Sparking in Detail

Filippenko and Radhakrishnan (1982) assumed that the sparking regions form discrete flux tubes which contain denser plasma than surrounding regions. Immediately prior to a discharge $\mathbf{E} \cdot \mathbf{B}$ in the gaps at the base of the flux tubes is greater than in surrounding regions, ensuring that sparks occur near sites of previous sparks. Discharges fill the flux tubes with plasma causing $\mathbf{E} \cdot \mathbf{B} = 0$ until new gaps form and the

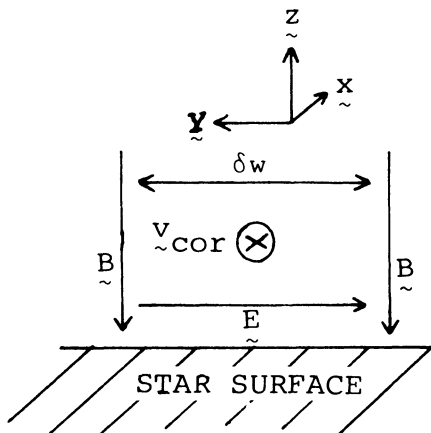


Figure 2. Field configuration in a flux tube near the star surface.

process is repeated. In Figure 2, the magnetic field lines drawn define opposite edges of the flux tube, which has an elongated elliptical cross-section (see Figure 4) and is extended in roughly the y-direction (see below, Section 5).

a) The Discharge Plasma

When the electron-positron plasma created in the gap comes into electrical contact with the star it experiences an \mathbf{E} field across its width as a result of the star's polarization. The plasma charge separates so as to make $\mathbf{E} = -(\Omega \mathbf{r}) \times \mathbf{B}$ continuous across the surface boundary (Figure 2). The manner in which this occurs is being investigated at present.

In modelling this we make the simplifying assumption that the charge separation generating \mathbf{E} can be treated as two surface charges at the position of the field lines forming opposite edges of the flux tube. The charges are separated by δw , the extent of the flux tube, as shown in Figure 2. We further treat these surface charges as single macrocharges which we refer to as charge bundles. The particles stream away from the star at $\approx c$ along the field lines and the divergence of field lines causes the separation between the charge bundles to increase. This changes the electric field they generate. The particles in a flux tube drift relative to the star with drift velocity (1) where we now interpret $\Delta \mathbf{E}$ in (1) as the difference between the actual electric field generated by the separated charge bundles at the top of the gap and the electric field required for corotation, $\Delta \mathbf{E} = \mathbf{E}_{act} - \mathbf{E}_{cor}$.

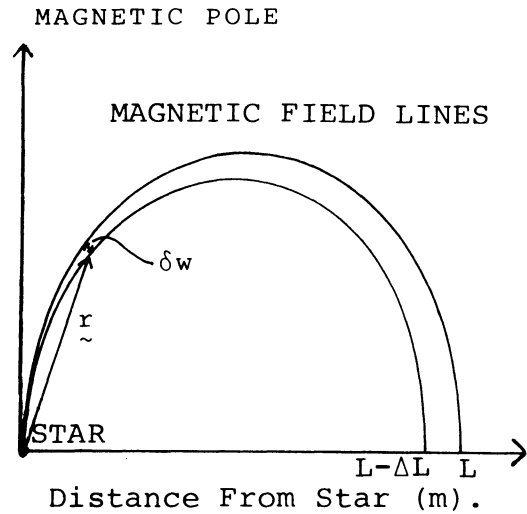


Figure 3. Magnetic field lines forming the plasma flux tube boundary.

Consider a thin flux tube close to the star with parameters as defined in Figure 3. The separation δw between one edge and the other can be calculated as a function of r , the distance from the centre of the star to the point in question, specifically,

$$\delta w \approx \frac{r^{3/2} \Delta L}{2L^{3/2}} \left(1 + \frac{r}{2L}\right) \quad (2)$$

Given the separation between the charged bundles, the variation of the electric field with distance r can be calculated

and thus ΔE can be calculated. Assuming that the distance Δx through which a flux tube drifts while the gap exists is small, and using the component directions as defined in Figure 2, one has

$$\Delta x = \int_0^h dx = \frac{1}{c} \int_0^h dz (\mathbf{v}_{ED})_x,$$

$$(\mathbf{v}_{ED})_x = \frac{\Delta \mathbf{E} \times \mathbf{B}}{|\mathbf{B}|^2}, \quad |(\mathbf{v}_{ED})_x| = \frac{|\Delta \mathbf{E}|}{|\mathbf{B}|}. \quad (3)$$

The distance h is the final gap height.

b) Results

The following calculations are for a one second period pulsar. A dipolar magnetic field is assumed with magnetic moment \mathbf{m} , of magnitude $1.5 \times 10^{27} \text{ Am}^2$ inclined at an angle of 30° to the rotation axis. The surface magnetic field is therefore of magnitude $B = 3 \times 10^8 \text{ T}$,

The magnetospheric gap grows at the speed of light and exists for a fraction $\sim 4.8 \times 10^{-2}$ of the time. The flux tube contains plasma down to the surface during the rest of the time and corotates.

The results for Δx calculated as a function of final gap height are shown in Table 1. The final column gives the number of degrees in longitude per period through which a flux tube drifts as a function of final gap height. Note that a negative drift rate indicates that the electric field present is less than that required for corotation, so the particles lag behind corotation and the subpulse drifts from the trailing edge to the leading edge of the pulse profile. In Table 2, observed drift rates for several pulsars are listed with the corresponding gap heights needed to explain them.

5. Discussion

With our model the implied drift rates are of the order of those observed; also the predominant drift is from the trailing to the leading edge of the pulse window as observed. These drift rates correspond to gap heights $\leq 300 \text{ m}$, which implies that the drift rates are imposed on the flux tubes near the surface of the star and not at heights where the radiation is emitted.

If the magnetic field lines do not twist immediately above the stellar surface, the electric field generated by the charge bundles as the gap forms continues to have the same direction

Table 1. Drift Rate vs Gap Height for a 1 second period pulsar and a 20m wide flux tube.

Gap Height (m)	Δx (mm)	Drift Rate (deg./period)
10	-0.12	-0.06
50	-0.59	-0.32
100	-1.21	-0.66
150	-1.86	-1.00
200	-2.53	-1.36
250	-3.23	-1.72

Table 2. Observed Drift Rates and Corresponding Gap Heights

Pulsar	P_1 (s)	Drift Rate (deg./period)	Gap Height (m)
*PSR 2016+28	0.558	-1.6	31
*PSR 1944+17	0.440	-1.3	17
*PSR 1933+16	0.359	-3.0	28
#PSR 0031-07	0.943	-1.6	14
		-1.3	125
		-1.4	135
		-1.8	175
		-2.0	195
#PSR 0809+74	1.29	-2.2	215
		-0.9	145
		-1.2	205

from

* Oster et.al. II, (1977)

Taylor et.al. (1975)

as the corotation electric field. Thus the formation of the magnetospheric gap causes a change in the magnitude of particle drift without altering its direction. The particles drift in this direction for $\Delta x \sim -1 \text{ mm}$ (see Table 1) before the next discharge event, when new charge bundles are created at the surface. The new charge bundles generate an electric field producing perfect corotation at the new position. As a result the drift path never deviates far from the corotation at emission radii, but patterns of drift across the magnetic polar cap established at the surface map simply onto those at emission altitudes. This implies that observations still reflect variations occurring near the surface.

The predicted drift rate across the profile is independent of distance from the magnetic pole. Although flux tubes at different distances from the magnetic pole drift through regions of slightly different magnetic field, for the dipole field assumed, the effect on the drift is not significant.

A strong point in favour of our model is that the gap heights required to explain observed drift rates agree well with those predicted in RS from a consideration of the electrodynamics of the plasma near the surface.

According to the model developed here subpulse drift should be universal and subpulses should be observed to drift right to the edge of the pulse window. In the RS model this is implied only if the line of sight from the Earth makes an almost tangential cut across the edge of the radiating hollow cone. Observations indicate that subpulse drift occurs across the entire window.

An important feature of the model is the shape of the flux tube, in particular the observation that the discharge at the base of the flux tube spreads in the direction opposite to the centre of curvature of the local magnetic field lines. During the time the gap is forming an order of magnitude calculation gives that the discharge spreads $\sim 30 \text{ m}$ (Cheng and Ruderman, 1980). This implies that subpulses at the edges of the pulse window should be wider than in the centre. We know of no observational evidence in support of this. The spreading

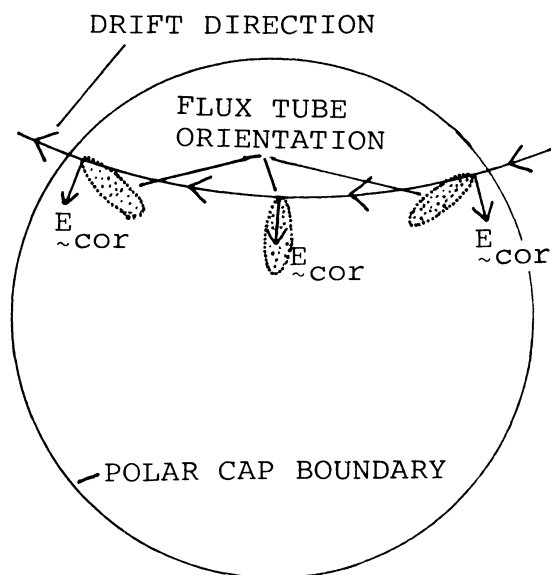


Figure 4. Drift path across the polar cap showing the direction of discharge spread at various positions.

of the discharge explains the observation that subpulse drift is more rapid at the edges of the pulse window. The direction of discharge spread is indicated in Figure 4 for several longitude positions. At the edges of the polar cap the charge separation generating E_{cor} is much harder to establish due to the orientation of the flux tube and perfect corotation may not occur. Thus the apparent drift may be much greater at the edges of the pulse window. When the line of sight makes a roughly central cut through the hollow cone emission profile, producing a double profile, there should be heavy overlapping of subpulses. This effect has been observed (Oster *et al.* III, 1977).

With our model one can also understand a number of features relating to changes in the subpulse drift rate. Some pulsars exhibit sudden and random changes in drift rate, e.g. PSR 0031-07, PSR 2021+51 (Taylor *et al.* 1975, Oster *et al.* II, 1977). A natural explanation for such changes can be developed by focussing on the gap height as the fundamental parameter determining drift rate. If the number of flux tubes in a region increases, the neutron star surface temperature rises and the final gap height attained before discharge increases (RS). Cheng and Ruderman (1977) derived the potential drop $\Delta V \propto f^{1/5}$, where f = fraction of the polar cap covered by flux tubes. When combined with the dependence (RS), $\Delta V \propto h^2$, this implies $h \propto f^{1/10}$ for a given pulsar. Assuming that the fraction of the polar cap filled by one sparking region is in the range $10^{-2}, 10^{-1}$ (RS) a change from one sparking region operating to two sparking regions operating would produce changes in the drift rate of around 6%, which is adequate to explain observed variations (cf. Table 2).

Pulse nulling is another type of pulse-to-pulse variation observed (Manchester and Taylor 1977 p. 36). Filippenko and Radhakrishnan (1982) explained nulls in terms of steady current being established for a while instead of discontinuous

discharges. The current to the surface is weaker during steady flow and thus the surface heating would be reduced. This explains why the drift rate is observed to be slower immediately after a null and only returns to its pre-null value after several periods when the surface has been heated up once more.

6. Conclusion

Our model of plasma behaviour near the surface of the star involves discharge sparking in discrete flux tubes, charge-separation of the discharge plasma to establish corotation and variation of the electric field generated as the plasma streams away from the surface along diverging field lines. Using the model we can account for properties such as i) observed drift rate, ii) direction of drift, iii) variation of drift rate across the profile, iv) sudden changes in drift rate of several subpulses at once, v) drift patterns observed in double profiles, vi) drift behaviour following nulls.

There are, however, several basic points in the model which cause us concern. These include the manner in which the charge separation needed for corotation is set up near the surface of the neutron star, and the way in which this is maintained for all but a fraction $\cong 1/20$ of the time. A more detailed investigation of the model is in progress.

- Bartel, N., Kardashev, N. S., Kuzmin, A. D., Nikolaev, N. Ya., Popov, M. V., Sieber, W., Smirnova, T. V., Soglasnov, V. A., and Wielebinski, R., *Astron. Astrophys.*, **93**, 85 (1981).
 Cheng, Andrew F., and Ruderman, M. A., *Astrophys. J.*, **214**, 598 (1977).
 Cheng, Andrew F., and Ruderman, M. A., *Astrophys. J.*, **235**, 576 (1988).
 Filippenko, Alexei, V., and Radhakrishnan, V., *Astrophys. J.*, **263**, 828 (1982).
 Goldreich, Peter and Julian, William, H., *Astrophys. J.*, **157**, 869 (1969).
 Manchester, R. N., and Taylor, J. H., *Pulsars*, W. H., Freeman and Company (1977).
 Oster, Ludwig and Sieber, Wolfgang, III, *Astrophys. J.*, **210**, 220 (1976).
 Oster, L., Hilton, D. A., and Sieber, W. I., *Astron. Astrophys.*, **57**, 1 (1977).
 Oster, Ludwig, Hilton, Douglas A., and Sieber, Wolfgang, II, *Astron. Astrophys.*, **57**, 323 (1977).
 Oster, Ludwig and Sieber, Wolfgang' III, *Astron. Astrophys.*, **58**, 303 (1977).
 Oster, L., and Sieber, W., IV, *Astron. Astrophys.*, **65**, 173 (1978).
 Oster, L., and Sieber, W., V, *Astron. Astrophys.*, **65**, 179 (1978).
 Ruderman, M. A., and Sutherland, P. G., *Astrophys. J.*, **196**, 51 (1975).
 Taylor, J. H., Manchester, R. N., and Huguenin, G. R., *Astrophys. J.*, **195**, 513 (1975).
 Wolszczan, A., *Astron. Astrophys.*, **63**, 425 (1978).
 Wolszczan, A., *Astron. Astrophys.*, **86**, 7 (1980).
 Wolszczan, A., Dartel, N., and Sieber, W., *Astron. Astrophys.*, **100**, 91 (1981).